Research Repository UCD

Title	On the sharpness of straight edge blades in cutting soft solids: Part I – indentation experiments
Authors(s)	McCarthy, Conor T., Hussey, M., Gilchrist, M. D.
Publication date	2007-09
Publication information	McCarthy, Conor T., M. Hussey, and M. D. Gilchrist. "On the Sharpness of Straight Edge Blades in Cutting Soft Solids: Part I – Indentation Experiments." Elsevier, September 2007. https://doi.org/10.1016/j.engfracmech.2006.10.015.
Publisher	Elsevier
Item record/more information	http://hdl.handle.net/10197/4909
Publisher's statement	This is the author's version of a work that was accepted for publication in Engineering Fracture Mechanics. Changes resulting from the publishing process, such as peer review, editing, corrections, structural formatting, and other quality control mechanisms may not be reflected in this document. Changes may have been made to this work since it was submitted for publication. A definitive version was subsequently published in Engineering Fracture Mechanics (74, 14, (2007)) DOI: http://dx.doi/org/10.1016/j.engfracmech.2006.10.015
Publisher's version (DOI)	10.1016/j.engfracmech.2006.10.015

Downloaded 2026-11-24 20:07:09

The UCD community has made this article openly available. Please share how this access benefits you. Your story matters! (@ucd_oa)

© Some rights reserved. For more information

On the Sharpness of Straight Edge Blades in Cutting Soft Solids: Part I - Indentation Experiments

C.T. McCarthy[1], M. Hussey, M.D. Gilchrist*

School of Electrical, Electronic & Mechanical Engineering, University College Dublin, Dublin 4, Ireland.

[1]Present Address: Department of Mechanical and Aeronautical Engineering, University of Limerick, Limerick, Ireland.

*Corresponding Author

Abstract

The sharpness of a blade is a key parameter in cutting soft solids, such as biological tissues, foodstuffs or elastomeric materials. It has a first order effect on the effort, and hence energy needed to cut, the quality of the cut surface and the life of the cutting instrument. To date, there is no standard definition, measurement or protocol to quantify blade sharpness. This paper derives a quantitative index of blade sharpness via indentation experiments in which elastomeric materials are cut using both sharp and blunt straight edge blades. It is found that the depth of blade indentation required to initiate a cut or crack in the target material is a function of the condition or sharpness of the blade's tip, and this property is used to formulate a so-called "blade sharpness index" (BSI). It is shown theoretically that this index is zero for an infinitely sharp blade and increases in a quadratic manner for increasing bluntness. For the blades tested herein, the sharpness index was found to vary between 0.2 for sharp blades and 0.5 for blunt blades, respectively. To examine the suitability of the index in other cutting configurations, experiments are performed using different blade types and target materials and it is found that the index is independent of the target material and thus pertains to the blade only. In the companion Part II to this paper a finite element model is developed to examine the effect of blade geometry on the sharpness index derived herein.

Keywords: materials mechanics, polymers, indentation, crack initiation, sharpness

NOMENCLATURE

dA	increment of newly created surface area
dU	strain energy
dx	increment of blade displacement
$d\Gamma$	work absorbed (energy dissipated) in remote plastic flow
$d\Lambda$	elastic strain energy stored during indentation
E	energy
F	applied force
h	length of cut surface
J_{Ic}	mode I fracture toughness
P	friction force
t	thickness of substrate material
u	blade displacement
X	force acting on blade
δ	depth of blade indentation

Subscripts

i	initiation

1. Introduction

The *sharpness* of a cutting instrument is a fundamentally important parameter in all cutting applications because it strongly influences the forces generated and hence energy required during the cutting process, as well as the life of the cutting edge, and surface finish or quality of the cut surface. A number of studies in diverse areas such as general surgery [1-3], forensic medicine [4-8], meat processing [9-13], zoology [14-15] and cutting tool evaluation [16] have loosely used the term *sharpness* to describe the performance of a cutting instrument. However, in these studies the definition of blade sharpness differs significantly. For example, in [1, 2, 9], sharpness is identified by a force level exerted by the cutting instrument during a cutting trial. [14-16] define sharpness as the radius of the cutting edge, while [3] define it by the power required to incise corneal tissue. There is, as yet, no acceptable definition for the sharpness of a cutting edge.

Despite the lack of standardisation, there are many industries in which blade sharpness plays an important role and affects not only the cutting process, but often has a direct influence on human life. In the medical industry, for example, studies have shown that a sharp scalpel blade will produce a wound of high quality, which will be less painful for the recovering patient, and will heal with less scaring than a blunt blade [17, 18]. These findings are in agreement with similar studies carried out using suturing needles [19, 20]. In the food processing industry, a number of studies conducted by McGorry et al. [9-11] have show that musculoskeletal disorders of the upper extremities could easily occur to workers using blades that are not sufficiently sharp.

A considerable number of studies have been carried out to measure the forces generated during cutting and piercing of soft solids [9, 20-22]. These force measurements

have been used in the development of robotic assisted surgery and minimally invasive surgery [20, 21], assessing the performance of scalpel blades [22] and investigating the force levels transmitted to butchers during routine meat cutting operations [9]. Common to all these studies is that a specialist cutting rig was developed, where the cutting instrument was pushed through a low stiffness substrate or target material, and the resulting forces measured with a load cell mounted either on the blade or the substrate fixing.

In forensic medicine, the assessment of force required to inflict a stab wound plays an important role [4, 5, 8], because the exact degree of this force is often the cause of disagreements in criminal proceedings regarding the murderous intent of an assailant, or the possibility that a victim accidentally fell against a weapon held in a fixed position by the assailant. It is extremely difficult to assess the force needed for penetrating a body because it is dependent on the sharpness of the weapon, nature of clothing, depth of wounds and type of tissue penetrated [4]. In a forensic suicide study, Ueno et al. [4] found that for a given blade impact energy, the sharpness of the tip was the most important factor in predicting skin penetration. This finding is in agreement with the works of Knight [6, 7] and Green [8], who described in detail the dynamics of stab wounds based on experiments on cadavers, and found that the sharpness of the tip of the weapon was the most important factor for penetration of skin.

A number of studies have considered the effect of cutting blade geometry on the forces generated during a cutting trial [11, 16, 23]. McGorry et al. [16] examined the effect of blade angles (ranging from 20 – 50 degrees) on cutting tool grip forces and moments exerted by professionals during two different meatpacking operations and found that blade angle did not have a significant effect on these measures. However, this finding is in disagreement with

the work of Moore et al. [23] who found, while carrying out cutting tests on sugar beet, that the cutting force increased as the wedge angle increased. Studies that have examined the effect of the cutting tool tip radius have found that as the radius increases, the cutting forces also increase [16, 24, 25].

The above studies highlight the need to accurately determine blade sharpness across very different fields of science and engineering. The fact that there is no standard definition, measurement or protocol to quantify the sharpness of a cutting instrument is largely due to the complexity and diversity of variables associated with cutting edge profiles [26]. However, a recent international standard addresses sharpness and proposes an edge retention test for cutlery [27]. This standard specifies the sharpness and edge retention of knives which are produced for professional and domestic use in the preparation of food of all kinds, specifically those knives intended for hand use. The standard describes a test procedure to evaluate blade "performance": the principle of the procedure is to reproduce a cutting action, by forward and reverse strokes, against a synthetic test medium under controlled parameters. The depth of cut produced by a 50 N load in the synthetic material per cutting cycle is used to evaluate the blade performance.

While this cutlery standard does provide a good starting point for a general definition of blade sharpness, much work is needed to investigate the fundamental mechanisms controlling the sharpness of a cutting instrument. Hence, the aim of this paper is to firstly propose a new definition of blade sharpness and subsequently quantify this measure for different blade types and target materials. In the companion Part II to this paper, a detailed finite element model is constructed to investigate the mechanics associated with indentation

type cutting. This model is subsequently used to examine the effect of blade geometry on the proposed sharpness index derived in this present paper.

2. Problem Description

This study is concerned with the analysis of indentation type cutting with straight edge blades. This cutting action is common to many processes such as chopping, slicing, carving and guillotining [26]. An idealisation of the indentation type cutting process is shown in Fig. 1. A blade is held perpendicular to a target or substrate material and pushed through it under an applied load F. The substrate material deforms initially to a penetration depth δ before cutting initiates. Depending upon the substrate material, this initial deformation can consist of both elastic and plastic components. Upon further loading, a cut or crack initiates, the substrate opens and the blade moves into this newly created volume. This process continues with increasing force until steady state cutting is established. The length of the cut surface is denoted by h and the substrate material thickness by t, as shown in Fig. 1. For the materials considered in this study, it should be noted that upon unloading, (i.e., retracting the blade) the initial deformation δ was generally fully recovered and the final cut length was equal to h.

Following a general procedure used in previous research in cutting soft solids [9, 20-22] as discussed above, the approach taken here in quantifying blade sharpness involves pushing a straight edge blade through a substrate material at a fixed velocity and observing the forces generated. Most of the experiments are performed using a No. 16 straight edged surgical scalpel blade, manufactured by Swann-Morton, as shown in Fig 2(a). This blade will subsequently be referred to as the SM blade. To examine the suitability of the proposed sharpness index to other blade types, a second set of experiments are performed using a razor

blade, manufactured by CAMB Machine Knives International (type CMK 152), as shown in Fig. 2(b). This blade will subsequently be referred to as the CAMB blade.

A 2.25 mm thick polyurethane sheet with a Shore hardness of 40 A was used as the cutting medium in most of the experiments. This material was chosen as it has a similar constitutive form to that of most soft bio-materials (i.e., a J-shaped stress-strain curve), thus rendering this analysis suitable for applications in cutting biological tissues. This polyurethane material will subsequently be referred to as the PU substrate. To investigate the independence of the proposed sharpness index on the substrate material used, additional cutting experiments were performed using a 1.6 mm thick silicone rubber sheet with a Shore hardness of 60 A. This material will subsequently be referred to as the SI substrate.

This paper is set out as follows. Firstly, indentation type cutting experiments are performed using sharp and blunt SM blades and PU substrates. The results from these tests are used to formulate a suitable criterion for a blade sharpness metric, and a corresponding sharpness index is then derived from first principles. The proposed index consists of a number of parameters which are necessarily determined by a series of experiments. The index is then calculated for sets of both sharp and blunt blades. Finally, to illustrate the generic applicability of this index to other cutting configurations, experiments are performed using different blade types and substrate materials.

3. Experimental Cutting Trials

The test rig used for the experimental cutting trials is shown in Fig. 3. The rig was connected to a 50 kN Tinius-Olsen universal testing machine. The lower part held the substrate material tightly between two anti-buckle guides. No pre-stress was applied to the

substrate. However, in order to minimise slipping, emery paper was inserted between the substrate and the clamps. The upper part of the rig held the blade via a blade handle (also by Swann-Morton) and the whole system was attached to the moving cross-head of the testing machine. Lake & Yeoh [28] carried out a study on cutting rubber sheets with razor blades and found that slow cutting rates produced relatively constant steady state cutting forces, while medium and fast rates produced a saw-tooth pattern, which was associated with a stick-slip behaviour caused by the substrate material splitting ahead of the blade. Following this study, in the experiments performed here the blade was pushed through the substrate material at a quasi-static rate of 10 mm/min. For a study on varying cutting rates, see [29]. The reaction force was measured by a 100 N load cell mounted above the blade clamp. Due to the relatively high rigidity of the blade clamping apparatus and low cutting forces observed, it was assumed here that the cross-head displacement was an accurate measure of the blade displacement and was thus used. The sampling frequency for both the load and displacement data was 6 Hz. The following sections describe the results from testing both sharp and blunt blades.

3.1 Sharp Blades

For this test series the term “sharp” refers to a virgin blade in an unused state. For each test, a new SM blade was removed from its protective packaging and fixed onto the blade handle of the test rig. For repeatability, three tests were performed and the corresponding load-deflection curves are shown in Fig. 4(a). As can be seen, all three curves rise initially in a non-linear manner to a blade displacement of approximately 2 mm. The three tests are in very close agreement up to this point. The curves then become linear until approximately 12 mm blade displacement. Again, good agreement is obtained in the linear region with only small differences in load and gradient being observed. After approximately 12 mm blade

displacement the loads become relatively constant and oscillate around the 30 N level, which is a result of using a quasi-static loading rate, as discussed above.

In order to examine the characteristics of the cutting process, the gradient of each load-deflection curve in Fig. 4(a) is plotted as a function of blade displacement in Fig. 4(b). These curves were generated by calculating the tangent modulus as a moving average of the values from twenty-seven adjacent pairs of data points in the load-deflection curve. This level of averaging was chosen as it sufficiently smoothed the initially noisy data, without masking any of the salient features of the cutting process.

The stiffness curves highlight some very interesting features of the cutting process. Firstly, they rise linearly up to approximately 2 mm blade displacement, at which point they become essentially constant. From a separate test in which the blade was progressively lowered in 0.05 mm increments and then retracted to allow the substrate to be examined, it was found that the point where the stiffness curves just deviate from linearity (i.e., Point A in Fig. 4(b)) corresponds to the point were a cut initiates in the substrate. It will be shown later that this point is, in fact, a function of the blade condition and can thus be used to formulate a blade sharpness metric. The level of blade indentation at the onset of cut formation is shown in Fig. 5. As can be seen, extensive deformation has occurred in the substrate, which is due to its highly elastic nature. This has significant relevance in the development of a finite element model in Part II of this paper, where a three-term Ogden [30] strain energy density function is needed to capture this non-linear material behaviour.

The locations marked A, B, C and D in Fig. 4(b) correspond to the cutting configurations shown schematically in Figs. 6(a), 6(b), 6(c) and 6(d), respectively. After the

cut initiates, the stiffness curves remain relatively constant (region B of Fig. 4(b)) until approximately 9 mm blade displacement. This region of constant stiffness represents the newly created cut surface passing over the side of the blade, as illustrated in Fig. 6(b). It should be noted that the blade height is 7 mm. After 9 mm blade displacement (i.e., $\delta + h = 2 + 7 = 9$ mm; see Fig. 1), the stiffness curves start to reduce (region C of Fig. 4(b)) and this region represents the onset of steady state cutting. This means that the initial portion of the newly formed cut surface has completely passed over the sides of the blade and re-contacted above the back of the blade, as shown in Fig. 6(c). After approximately 16 mm blade displacement, the stiffness curves approach zero stiffness (region D of Fig. 4(b)) and this represents the point where steady state cutting is fully established, i.e., where the cutting forces become constant (around a mean value of approximately 30 N), as shown in Fig. 4(a). During steady state cutting the blade and substrate reach an equilibrium state, as illustrated in Fig. 6(d).

3.2 Blunt Blades

Following the same procedure, a series of tests were carried out with a new blade being used for each repeat of the test. However, differently from the sharp blade tests of Section 3.1, each blade was artificially blunted by lightly rubbing a strip of fine silica glass paper (180 Grit) along the tip of the blade, in a direction parallel to the blade handle. One pass was sufficient to blunt the blade. The corresponding load-deflection and stiffness plots for these cutting tests are shown in Figs. 7(a) and 7(b), respectively. The load-deflection response for each test shows excellent agreement until approximately 22 mm blade displacement, after which Test 1 shows a severe downturn. This was due to the substrate material buckling out of plane in a wrinkling type manner, causing the material to bend rather than be cut. This phenomenon was also observed by Lake & Yeoh [28] when cutting rubber sheets with blunt knives.

As can be seen in Fig. 7(a), the load-deflection responses for the blunt blades are considerably different in form and magnitude to those of the sharp blades (Fig. 4(a)). However, initially the blunt set of curves (Fig. 7(a)) are identical to the sharp set (Fig. 4(a)), and both display a non-linear behaviour associated with the indentation process before the cut initiates in the substrate. Turning to Fig. 7(b), it can be seen that the stiffness plots for the blunt blades rise in an essentially linear manner until approximately 4 mm blade displacement (Point E, Fig. 7(b)) at which point they rapidly drop off to zero stiffness before rising again. It was found in separate retraction experiments (again, by lowering and retracting the blade in small increments to inspect the substrate surface) that Point E corresponds to (as with Point A for the sharp blades) the point where the cut initiates in the substrate. Hence, it has been found that the point where the stiffness plot just deviates from linearity corresponds to the point where a cut initiates in the substrate.

However, clearly Point E in Fig. 7(b) occurs at a considerably higher blade displacement and load level than that of Point A in Fig. 4(b) for the sharp blades. As the testing conditions were identical (apart from the condition of the blade tip) for both sets of experiments, it can be concluded that the point where a cut initiates in the substrate is a function of the condition of the blade tip or the "sharpness" of the blade. This point can thus be used to formulate a blade sharpness metric.

4. Derivation of a Sharpness Metric

Before deriving a new sharpness metric, it is important to state some axioms which such a criterion should meet. First and foremost, such a metric should clearly identify differences between sharp and blunt cutting edges. Second, it should ultimately pertain to the blade only, and not be affected by the substrate material. Third, it should be related to the

mechanics of the cutting process, such as mode of opening of the substrate; this is necessary in order to distinguish between different types of cutting processes, such as those characterised by mode I, II and III fracture mechanisms. Finally, it should be intuitive and easily obtained from experimental data or analysis.

As discussed in Section 3 above, the point where a stiffness plot first deviates from linearity corresponds to the point where a cut initiates in the substrate. This point is a function of the condition or sharpness of the blade tip and can be uniquely determined from the amount of blade displacement required to initiate a cut in the substrate. By mapping back to the load-deflection curve, the energy required to initiate a cut in the substrate can be determined. It is postulated here that this energy can be used to quantify differences between sharp and blunt cutting edges. This energy, referred to here as the "cut initiation energy" or E_i, can be obtained by integrating the load-deflection curve from the start of the test up to the point where a cut or crack just initiates in the substrate, i.e.,

$$E_i = \int_{\delta_i} F dx \qquad \textbf{(1)}$$

where: F is the cutting force, dx is an increment of blade displacement in the loading direction (see Fig. 1 for coordinate system used) and δ_i is the blade displacement or indentation depth at which a cut initiates in the substrate. This blade displacement δ_i is determined from Points A and E in Figs. 4(b) and 7(b) for sharp and blunt blades, respectively.

The cut initiation energy, E_i, is dependent on the thickness of the substrate used. In order to eliminate this dependency, the cut initiation energy is normalised with respect to the substrate thickness. Hence, a cut initiation energy per unit thickness, E_i^* is defined as:

$$E_i^* = \frac{\int_{\delta_i} F dx}{t} \tag{2}$$

where: t is the thickness of the substrate, as shown in Fig. 1. It is important to consider the substrate material in any sharpness metric, but ultimately such a metric should pertain to the blade only since the blade's intended function is in general, not known *a priori*. The influence of the substrate material can be introduced by normalising the cut initiation energy per unit thickness (i.e., Eq. 2) by the substrate's fracture toughness, i.e.,

$$\overline{E}_i^* = \frac{\int_{\delta_i} F dx}{t J_{ic}} \tag{3}$$

where: $\overline{E}_i^*$ is the normalised cut initiation energy per unit thickness of substrate and J_{ic} is the Mode i fracture toughness of the substrate. For this analysis the opening mode (i.e., Mode I) fracture toughness, J_{Ic}, would be used, as this is the mode in which the substrate is being cut. However, normalising with respect to the mode of fracture allows this particular metric to be used for other cutting modes such as scissors cutting, which produces a tearing Mode III fracture [31, 32] or a combined opening tension and sliding shear Mode I/II, present when hand carving meat with a knife, for example.

Finally, it is further hypothesised that the sharpness of a blade is inversely proportional to the indentation depth to initiate a cut or crack in the substrate, δ_i. This postulate is suggested by the results of the experiments performed in Section 3, where it was found that the sharp (i.e., new) blades required approximately 2 mm indentation to initiate a cut, while the blunt blades required approximately 4 mm. Hence, a measure for blade sharpness, or more appropriately a blade sharpness index or *BSI,* can now be written as:

$$BSI = \frac{\int_{\delta_i} F dx}{\delta_i t J_{ic}} \tag{4}$$

This metric relates the energy required to initiate a cut in the substrate to the substrate's fracture toughness and thickness and to the indentation depth of cut formation. The numerator is a scalar energy quantity, while the dominator is related to the material, geometric and indentation depth to fracture of the substrate, thus providing a simple formulation to evaluate blade sharpness. It should be noted that the sharpness index of Eq. 4 is a dimensionless quantity.

5. Blade Sharpness Index Evaluation

In this section the parameters of the BSI (Eq. 4) are first evaluated using test data from Section 3. Additional tests are also necessary to determine some BSI parameters and these are described. The BSI is then calculated for different blades and substrates.

5.1 Evaluation of δ_i

As discussed previously, the blade displacement required to initiate a cut in the substrate, i.e. δ_i, can be determined by progressively lowering the blade into the substrate and then retracting it to examine the substrate surface for evidence of cut formation. However, it was found that this point corresponds to the point where the stiffness curves just deviate from linearity. Hence, δ_i was determined for both the sharp and blunt blades from the stiffness plots of Figs. 4(b) and 7(b), respectively, and the results for these tests are summarised in Table 1.

5.2 Evaluation of E_i

After determining δ_i, the cut initiation energy E_i can be determined by integrating the load-deflection response from a cutting experiment from the start of the test (i.e., where the

load just starts to rise) up to δ_i. This was done by numerically integrating the load-deflection test data of Section 3 according to the following equation:

$$E_i = \int_{x_0}^{\delta_i} F dx \approx \frac{1}{2}\sum_{j=1}^{N} F_j\left(x_{j+1} - x_{j-1}\right) \quad \textbf{(5)}$$

where: F_j and x_j are the force and displacement values at experimental data point j, respectively, x_o is the displacement where the force just starts to rise and N is the total number of data points up to cut initiation. Table 1 lists the results for the cut initiation energies E_i for each test.

5.3 Experiments to Determine Mode I Fracture Toughness, J_{Ic}

This paper is concerned with the sharpness of blades for applications in cutting soft solids. Due to the very ductile nature of these materials, it is difficult to determine their fracture toughness using standard fracture toughness tests. One approach that has been used to evaluate the fracture toughness of "soft" solids such as biological materials and foodstuffs is to carry out a cutting test [31-33].

A recent paper by Doran et al. [31] proposed a simple model to determine the fracture toughness of thin biological membranes. The approach used was to transversely load a thin strip of chicken skin and then force a surgical blade through it. The resulting load-deflection characteristics were used to calculate the fracture toughness J_{Ic} or the so called "resistance to fracture" using the following equation:

$$J_{Ic} = \frac{\left(Xu - d\Lambda\right) + dU - d\Gamma}{dA} \quad \textbf{(6)}$$

where: X is the force acting on the blade and u is the blade displacement. The term $d\Lambda$ represents the elastic strain energy stored in the membrane during indentation (i.e., before cutting initiates), dU represents the strain energy stored in the substrate, $d\Gamma$ represents the

work absorbed in remote plastic flow and dA is an increment of newly created surface area due to cutting. As a starting point, this model is adopted here in an attempt to determine the Mode I fracture toughness of the PU substrate material.

The experimental cutting rig described in Section 3 was used to carry out the cutting trials to determine the PU fracture toughness. This rig is similar in functionality to that used by [31]. However, it does not induce any transverse loading into the substrate material, and as a result the stored strain energy term dU in Eq. 6 is zero. However, a consequence of not applying any transverse pre-stress is that the substrate material remains in contact with the sides of the blade during cutting, as illustrated in Fig. 6. Hence, energy is dissipated due to friction between the sides of the blade and the substrate. To account for this, Eq. 6 is modified to include energy dissipation due to friction, Pu:

$$J_{Ic} = \frac{Xu - d\Lambda - Pu - d\Gamma}{dA} \tag{7}$$

where: P is the total friction force acting between the blade and substrate.

Doran et al. [31] stated that if a sharp blade is used during the test, the level of remote (from the tip) plastic flow can be regarded as negligible and $d\Gamma$ can be ignored. In the experiments performed here, when the blade was retracted after cutting, the substrate material returned to its initial position without any apparent plastic deformation. Hence, it was assumed here that the energy dissipated due to plastic flow, $d\Gamma$, was negligible and so this term in Eq. 7 was ignored.

If the analysis is confined to a region where steady state cutting is occurring, the energy due to initial indentation $d\Lambda$ can be ignored since this energy is restored elastically when the blade is retracted. From the cutting trials carried out in Section 3, it was found that

steady state cutting started at approximately 16 mm blade indentation for sharp blades. Hence for this analysis, only experimental information after 16 mm blade indentation is considered in the calculation of J_{Ic}. The final equation used to calculate J_{Ic} is:

$$J_{Ic} = \frac{(X - P)u}{dA} \tag{8}$$

with the caveat that it is only valid if the analysis is confined to a region of steady state cutting. Otherwise, the $d\Lambda$ term must be considered. The product Xu in Eq. 8 can be determined by integrating the load-displacement curve obtained from a cutting trial. An additional set of cutting experiments to those reported in Section 3 were carried out to measure J_{Ic} and a typical load-deflection curve is shown in Fig. 8.

An approach used to estimate the energy due to friction when determining the Mode III fracture toughness of a soft biological tissue using a scissors cutting test [32] was to first carry out a cutting test, and then repeat this test with the cut substrate still in place. In this way, all test parameters are identical to the initial cutting trial except that in the second or free pass no energy is needed to cut the material, since it has been cut previously in the cutting pass. In this way, the energy due to friction can be determined. Brown et al. [34] used a similar approach to determine the friction forces generated when cutting foodstuffs. Following these studies, it was decided to adopt this approach in order to determine the friction energy term, Pu in Eq. 8. The approach taken here was to first carry out a cutting experiment as normal. The blade was then retracted after the cutting pass and the substrate material allowed to settle back to its initial position. Finally, the experiment was repeated with the cut substrate left in the lower part of the test rig and the load-displacement data was recorded. Fig. 8 shows the results from this free pass and it can be seen that significant force and hence energy is needed to push the blade though the pre-cut material. The area under this curve determines the energy dissipated due to friction. By differencing the load-deflection

curves for the cutting pass and the free pass, the *(X-P)* term in Eq. 8 can be determined as a function of blade displacement and this is also plotted in Fig. 8.

The term *(X-P)u* in Eq. 8 is the area under the difference curve *(X-P)* in Fig. 8 and can be evaluated by integrating this curve with respect to the blade indentation depth. This was achieved here by integrating the test data using an equation similar to Eq. 5. However, to avoid the $d\Lambda$ term in Eq. 7 the integration must exclude the initial indentation energy and this was achieved by only considering the portion of the curve representing steady state cutting (i.e., 16 mm blade displacement onwards). The resulting *(X-P)u* term is plotted as a function of the cut area *dA* in Fig. 9 for three repeats of the tests. The cut area was determined by:

$$dA = 2ht \tag{9}$$

where: t is the thickness of the substrate (which is 2.25 mm for the PU material), h is the length of the cut and the factor 2 represents the new surfaces that are created on the two sides of the blade. Following Eq. 8 and Fig. 9, the fracture toughness J_{Ic} is obtained from the slope of best-fit linear curves to this data and the resulting values are shown Table 2.

5.4 Evaluation of Blade Sharpness

At this point, all the necessary data to calculate the BSI (Eq. 4) for the sharp and blunt blades have been determined and are listed in Table 1. However before doing so, a closed form expression for the BSI is derived in order to help understand its attributes. By examining the initial portion of the load-displacement curve (i.e., from 0 to δ_i) for both the sharp and blunt blades in Section 3, it was found that they can be represented almost exactly by the following closed form expression:

$$F = Ax^2 + Bx \tag{10}$$

where: F is the load, x is the blade displacement and A and B are both empirical constants (and are equal to 0.24 N/mm^2 and 1.44 N/mm for the PU substrate, respectively, regardless of whether the blade is sharp or blunt). Substituting Eq. 10 into Eq. 4 and carrying out the integration yields the following closed-form expression for the blade sharpness index:

$$BSI = \frac{2A\delta_i^2 + 3B\delta_i}{6tJ_{Ic}} \quad \textbf{(11)}$$

From this equation, it can be seen that the BSI is a quadratic function of blade indentation depth to cut initiation δ_i. For an infinitely sharp blade, δ_i would tend towards zero, i.e., $\delta_i \to 0$ and so, in the limit the BSI would equal zero (i.e. $Lim(BSI)_{\delta_i \to 0} = 0$). Hence, for an infinitely sharp blade the BSI would be zero, thus providing a lower bound. The BSI is unbound for $\delta_i > 0$ and so increasing values of BSI represent increasing levels of blade bluntness.

By entering the parameters listed in Table 1 into Eq. 4 the BSI was determined for both the sharp and blunt blades, and the results are also listed in Table 1. The average BSI value for the sharp SM blade is 0.216 with a standard deviation of 0.016, while the average value for the blunt blade is 0.514 with a standard deviation of 0.012. The sharp blades produce a lower BSI than the blunt blades, as expected, and they differ by a factor of approximately 2.4. It should be noted that the BSI scale is non-linear. However, for the BSI range measured here ($0.216 \le BSI \le 0.514$), the linear term in Eq. 11 dominates since the B coefficient is six times greater than the A coefficient (A = 0.24 N/mm^2, B = 1.44 N/mm), and so the BSI suggests that the sharp blades are approximately 2.4 times more effective than the blunt blades.

In Part II of this paper a finite element model is used to investigate the effect of different blade geometric factors, such as wedge angle and tip radius, on the blade sharpness index and so a discussion on this aspect is omitted here.

5.5 Verification of Substrate Independence

For this study, silicone (SI) rubber was procured from a local prosthetic implant manufacturer and used as the substrate material in a new set of experiments. These experiments were carried out in order to demonstrate that the BSI is independent of the substrate material used. The composition for the SI material was a standard formulation of polydialkylsiloxane propane, as used in the medical device industry [35]. It had a Shore hardness of 60A and a thickness of 1.6 mm. Following identical procedures to those outlined in Section 3, this sharpness study yielded the results shown in the last rows of Table 1. The first thing to note is that the indentation depth to cut initiation, δ_i, is considerably lower than that for the PU substrate, and as a result the cut initiation energy, E_i, is also considerably lower. The fracture toughness for this material was determined following the procedure outlined in Section 5.3 and the results are listed in Table 2. The average value of this fracture toughness is in broad agreement with values for Sil8800 and B452 type silicone rubbers obtained using a trouser tear test [36], thus verifying the validity of the current approach.

The results for the BSI when cutting the SI substrate are listed in Table 1. The average BSI value is 0.216 with a standard deviation of 0.018. This value is, on average, very close to that obtained when cutting the PU substrate, thus demonstrating that the BSI is independent of the substrate used, at least for the two material types examined here.

5.6 Application to Other Blade Types

In order to show that the BSI is generically applicable to other blade types, experiments were performed using a CAMB blade to cut a PU substrate. These blades are designed differently to the surgical scalpel blades used thus far, and have an aluminum spine on the back of the blade (as shown in Fig. 2(b)) for fixing, rather than a slot for a blade handle as used in the fixing of SM blades. As a result, the sharpness-testing rig shown in Fig. 3 had to be modified in order to test these razor blades.

Following the procedure outlined in Section 3, a set of new CAMB razor blades were tested against the PU substrate and the results are shown in Table 3. Differently from before, seven repeats of the test were performed. It should be noted that the load deflection curve for these blades was very similar to that for the SM blades. However, it can be seen in Table 3 that δ_i for this blade is approximately 0.3 mm greater than that for the SM blade and, as a result, E_i is higher. Consequently the BSI for this blade is higher by a factor of approximately 1.16, indicating that the SM blade is a sharper instrument.

To investigate this hypothesis, the reaction forces for SM and CAMB blades are examined at 2 mm blade displacement (i.e., δ_i for the SM blade) and the results are listed in Table 1 and Table 3, respectively. As can be seen, there is virtually no difference in the loads at this displacement level for both types of blade. This highlights that the proposed BSI can distinguish between blades that produce similar load levels, but have different levels of indentation to cause a cut to initiate in a substrate, thus suggesting that force alone is not a complete indicator of blade sharpness, as currently used in a number of professional areas.

6. Discussion and Conclusion

This paper has set out to develop a new measure or metric for quantifying the sharpness of a blade for applications in cutting soft solids. This index may be useful in a wide range of applications, including the meat processing industry, general surgery, forensic medicine, zoology, and some machining processes.

The blade sharpness index, or BSI, was derived by means of a set of experiments where sharp (or new) and blunted straight edged No. 16 Swann-Morton scalpel blades were forced through a polyurethane elastomeric substrate at a constant velocity. By plotting the slope of the force-displacement curves from these tests as a function of blade displacement, it was found that the point where a cut initiates in the substrate corresponds to the point where the stiffness plots first deviate from linearity, and that this point is a function of the condition or sharpness of the blade tip.

Following these experiments, a blade sharpness index was derived based on the energy and blade indentation depth required to initiate a cut in the substrate material, and on the substrate's fracture toughness and thickness. This dimensionless index was evaluated for both the sharp and blunt blades and had an average value of 0.217 and 0.514, respectively. By writing closed form expressions for the force acting on the blade as a function of blade displacement, it was possible to determine a closed form expression for the BSI. By examining this expression, it was shown that the BSI varies in a quadratic manner with blade indentation depth to cut formation, δ_i, thus highlighting that the BSI scale is non-linear. It was also possible to theoretically determine the BSI index for an infinitely sharp blade by assuming that δ_i for such a blade would approach zero, and hence in the limit the BSI would be also be zero. This provided a lower bound for the sharpness index and suggests that the closer the BSI is to zero the sharper the blade is. The closed-form expression used here was

based upon experimental results using a polyurethane substrate, which is unlikely to be valid for other substrate materials. However, once the load deflection curve can be expressed as a first or higher order polynomial in blade displacement, x, then the BSI $\rightarrow 0$ as $\delta_i \rightarrow 0$ for all substrate materials.

It was postulated that the BSI should be independent of the substrate material used, and should thus only pertain to the blade. This was shown to be true for the polyurethane and silicone substrates tested. However, the question arises "Is a blade that is considered sharp when cutting a soft solid, such as natural rubber or skin, for example, still sharp when required to cut a metallic material, such as steel or aluminum?". It is quite obvious that any blade designed to cut a soft solid would be completely inadequate to cut a metal for any significant length of time, if at all. However, to answer this question, one must consider the micromechanical deformation that takes place at the blade's tip during cutting. If the material properties, such as stiffness, strength, fracture toughness and hardness are comparable between the blade and substrate, extensive plastic deformation will occur at the blade's tip (due to the high concentration of stress at that point), before δ_i is reached in the substrate. As a result, the geometry of the blade tip would flatten out to a point where the physics of the problem would change from a cutting phenomenon to a contact phenomenon. By using the BSI, it would appear then that the blade is blunt, since it would now take a significant amount of energy to reach δ_i (if attained at all). However, this blunting occurs as a result of the measurement process and not because the blade was initially blunt. Hence, blade sharpness is independent of the substrate used, but in order to measure it, the material properties of the substrate should be orders of magnitude less than that of the blade, so as to avoid changing the geometry of the blade tip.

Some approaches in determining the performance of a blade require that the blade undergo a significant amount of cutting and this obviously leads to some degradation of the blade's cutting edge. The approach developed herein has the advantage that the blade is only required to indent the substrate once by a small amount, thus minimising wear on the blade. This approach, therefore, may be useful to blade manufacturers when carrying out quality control tests before sending blades out to market.

Finally, this paper has not considered the effect of blade geometry, such as wedge angle, tip radius or surface finish on the BSI. Manufacturing one-off blades with custom designed geometric ratios would be extremely difficult and expensive and is outside the scope of this paper. However, to overcome this, a finite element model is developed in Part II of this paper and used to investigate the effect that these geometric factors have on the proposed BSI.

7. Acknowledgements

The authors gratefully acknowledge Enterprise Ireland for funding this research under the auspices of the Commercialisation Fund (ATRP/2002/422B).

8. References

[1] Watkins FH, London SD, Neal JG, Thacker JG, Edlich RF. Biomechanical performance of cutting edge surgical needles. J. Emerg. Med. 1997;15(5):679-685.

[2] Thacker JG, Rodeheaver GT, Towler MA, Edlich RF. Surgical needle sharpness. The American Journal of Surgery. 1989;157(3):334-339.

[3] Huebscher HJ, Gober GJ, Lommatzsch PK. The sharpness of incision instruments in corneal tissue. Ophthal. Surg. 1989;20(2):120-123.

[4] Ueno Y, Asano M, Nushida H, Adachi J, Tatsuno Y. An unusual case of suicide by stabbing with a falling weighted dagger. Forensic Sci. Int. 1999;101(3):229-236.

[5] O'Callaghan PT, Jones MD, James DS, Leadbeatter S, Evans SL, Nokes LDM. A biomechanical reconstruction of a wound caused by a glass shard: A case report. Forensic Sci. Int. 2001;117(3):221-231.

[6] Knight B. The dynamics of stab wounds. Forensic Sci. 1975;6(3):249-255.

[7] Knight B. Forensic Pathology. Hodder Education, 2004.

[8] Green MA Stab wound dynamics: A recording technique for use in medico-legal investigations. J. Forensic Sci. 1978;18(3-4):161-163.

[9] McGorry RW, Dowd PC, Dempsey PG. Cutting moments and grip forces in meat cutting operations and the effect of knife sharpness. Appl. Ergon. 2003;34(4):375-382.

[10] McGorry RW, Dowd PC, Dempsey PG. A technique for field measurement of knife sharpness. Appl. Ergon. 2005;36(5):635-640.

[11] McGorry RW, Dowd PC, Dempsey PG. The effect of blade finish and blade edge angle on forces used in meat cutting operations. Appl. Ergon. 2005;36(1):71-77.

[12] King MJ. Knife and impact cutting of lamb bone. Meat Sci. 1999;52(1):29-38.

[13] Bishu RR, Calkins C, Lei X, Chin A. Effect of knife type and sharpness on cutting forces. Advances in Occupational Ergonomics and Safety. 1996;2:479-483.

[14] Popowics TE, Fortelius M. On the cutting edge: Tooth blade sharpness in herbivorous and faunivorous mammals. Ann. Zool. Fennici. 1997;34:73-88.

[15] Evans AR. Connecting morphology, function and tooth wear in microchiropterans. Biological Journal of the Linnean Society. 2005;85(1):81-96.

[16] Yuan JJ, Zhou M, Dong S. Effect of diamond tool sharpness on minimum cutting thickness and cutting surface integrity in ultraprecision machining. J. Mater. Process. Tech. 1996;62(4):327-330.

[17] Black D, Marks R, Caunt A. Measurement of scalpel blade sharpness and its relationship to wound healing. Bioengineering Skin. 1985;1**:**111-123.

[18] Izmailov GA, Orenburov PI, Repin VA, Gorbunov SM, Ismailov SG. Evaluation of the healing of skin wounds inflicted by steel scalpels with various levels of sharpness. Khirurgiia (Mosk). 1989;6:75-78.

[19] Towler MA, Rodeheaver GT. Influence of cutting edge configuration on surgical needle penetration forces. J. Emerg. Med. 1988;6(6):475-481.

[20] Frick TB, Marucci DD, Cartmill JA, Martin CJ, Walsh WR. Resistance forces acting on suture needles. J. Biomech. 2001;34(10):1335-1340.

[21] Tholey G, Chanthasopeephan T, Hu T, Desai JP, Lau A. Measuring grasping and cutting forces for reality-based haptic modeling. International Congress Series, 2003;1256:794-800.

[22] Santhanam R, Valenta HL. Cutting force measurement platform for quantitative assessment of surgical cutting instruments. Biomed. Sci. Instrum. 1996;32:237-243.

[23] Moore MA, King FS, Davis PF, Manby TCD. The effect of knife geometry on cutting force and fracture in sugar beet topping. J. Agr. Eng. Res. 1979;24(1):11-27.

[24] Meehan RR, Kumar J, Earl M, Svenson E, Burns SJ. Role of blade sharpness in cutting instabilities of polyethylene terephthalate. J. Mat. Sci. Lett. 1999;18(2):93-95.

[25] Goh SM, Charalambides MN, Williams JG. On the mechanics of wire cutting of cheese. Eng. Fract. Mech. 2005;72(6):931-946.

[26] Reilly GA, McCormack BAO, Taylor D. Cutting sharpness measurement: A critical review. J. Mat. Process. Tech. 2004;153-154:261-267.

[27] ISO International Standard Materials and articles in contact with foodstuff –Cutlery and table hollowware. Part 5: Specification for sharpness and edge retention test of cutlery. ISO 8442-5:2004(E), 2004.

[28] Lake GJ, Yeoh OH. Measurement of rubber cutting resistance in the absence of friction. Int. J. Fract., 1978;14(5):509-526.

[29] McCarthy CT, O'Dwyer E, Hussey M, Gilchrist MD, O'Dowd NP. A numerical and experimental investigation into the forces generated when cutting biomaterials. Medical Device Materials II, Proceedings of the Materials & Processes for Medical Devices Conference, August 25-27, 2004, St. Paul, Minnesota, USA, M. Helmus and D. Medlin, Ed., ASM International, 2005, p 140-145.

[30] Ogden RW. Large deformation isotropic elasticity: On the correlation of theory and experiment for incompressible rubberlike solids. Proc. R. Soc. Lond. A. 1972;326:565-584.

[31] Doran CF, McCormack BAO, Macey A. A simplified model to determine the contribution of strain energy in the failure process of thin biological membranes during cutting. Strain. 2004;40(4):173-179.

[32] Pereira BP, Lucas PW, Swee-Hin T. Ranking the fracture toughness of thin mammalian soft tissues using the scissors cutting test. J. Biomech. 1997;30(1):91-94.

[33] Atkins AG. Toughness and cutting: A new way of simultaneously determining ductile fracture toughness and strength. Eng. Fract. Mech. 2005;72(6):849-860.

[34] Brown T, James ST, Purnell GL. Cutting forces in food: Experimental measurements. J. Food Eng. 2005;70(2):165-170.

[35] Compton RA. Silicone manufacturing for long-term implants. J. Long-term Effects of Medical Implants, 1997;7(1):29-54.

[36] Shergold OA, Fleck NA. Mechanisms of deep penetration of soft solids, with application to the injection and wounding of skin. Proc. R. Soc. Lond. A. 2004;460:3037-3058.

FIGURE CAPTIONS

Figure 1: An idealisation of the indentation type cutting process.

Figure 2: Photographs of the blades used in this study, (a) SM Scalpel Blade, (b) CAMB Razor Blade.

Figure 3: Experimental rig used for the cutting trials.

Figure 4: Indentation cutting with sharp SM blades; (a) Load-deflection curves, (b) corresponding stiffness-deflection curves.

Figure 5: Photograph showing the level of blade indentation at the point of cut formation in the substrate.

Figure 6: Different stages of the indentation cutting process; (a) Initial indentation at the point of cut formation, (b) Intermediate cutting where the cut material travels up the side of the blade, (c) onset of steady state cutting where the substrate material re-contacts above the back of the blade, (d) Steady state cutting, (a), (b), (c) and (d) correspond to locations A, B, C and D of Fig. 4(b).

Figure 7: Indentation cutting with blunt SM blades; (a) Load-deflection curves, (b) corresponding stiffness-deflection curves.

Figure 8: Load-displacement curves for a cutting pass (X), a free pass (P) and the difference (X-P).

Figure 9: $(X\text{-}P)u$ term as a function of cut area dA.

Table 1 Experimental data for evaluating the BSI for SM blades

Substrate Material	Blade Condition	Test No.	δ_i (mm)	F at δ_i (N)	E_i (N mm)	t (mm)	J_{Ic} (kJ m^{-2})	BSI
PU	Sharp	1	2.03	4	3.87	2.25	3.67	**0.231**
		2	1.97	3.76	3.58			**0.219**
		3	2.08	3.6	3.41			**0.200**
	Blunt	1	4.07	9.9	17.65			**0.526**
		2	4.10	9.5	17.04			**0.504**
		3	4.07	9.6	17.05			**0.512**
SI	Sharp	1	0.43	0.98	0.257	1.6	1.85	**0.202**
		2	0.44	0.92	0.273			**0.210**
		3	0.44	0.99	0.3082			**0.237**

Table 2 J_{Ic} values for the PU and SI substrates

Material	Test No.	J_{Ic} (kJ m^{-2})	Average	Standard Deviation
PU	1	3.816	3.67	0.172
	2	3.481		
	3	3.713		
SI	1	1.974	1.85	0.118
	2	1.739		
	3	1.850		

Table 3 Experimental data for evaluating the BSI for sharp CAMB razor blades

Substrate Material	Test No.	δ_i (mm)	F at δ_i (N)	F at 2 mm (N)	E_i (Nmm)	t (mm)	J_{Ic} (kJ m^{-2})	BSI	BSI Ave. (S.D.)
PU	1	2.32	4.48	3.78	4.77	2.25	3.67	**0.249**	**0.251 (0.006)**
	2	2.34	4.6	3.9	4.92			**0.255**	
	3	2.32	4.56	3.86	4.88			**0.255**	
	4	2.31	4.48	3.8	4.84			**0.254**	
	5	2.28	4.18	3.54	4.52			**0.241**	
	6	2.34	4.4	3.73	4.75			**0.246**	
	7	2.27	4.35	3.78	4.83			**0.258**	

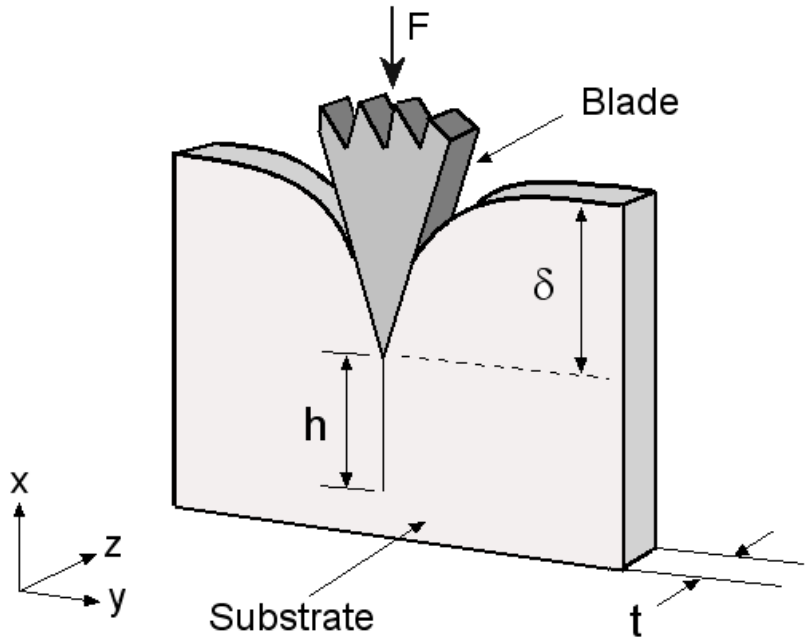

Figure 1 An idealisation of the indentation type cutting process

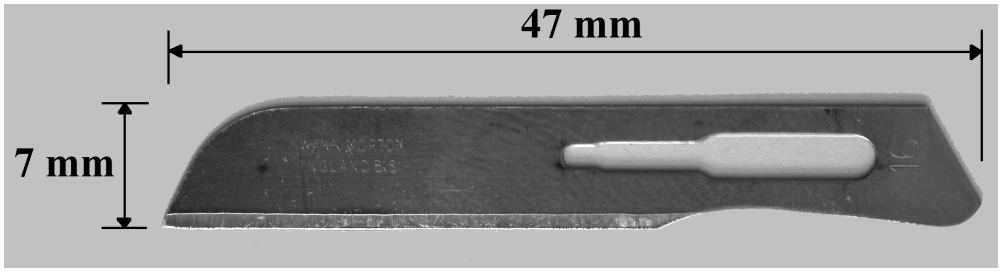

(a)

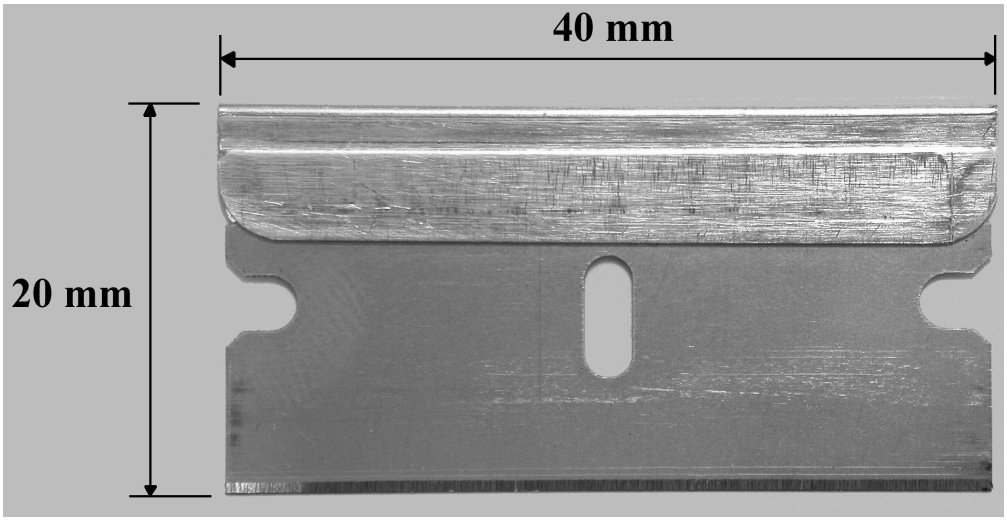

(b)

Figure 2 Photographs of the blades used in this study, (a) SM Scalpel Blade, (b) CAMB Razor Blade

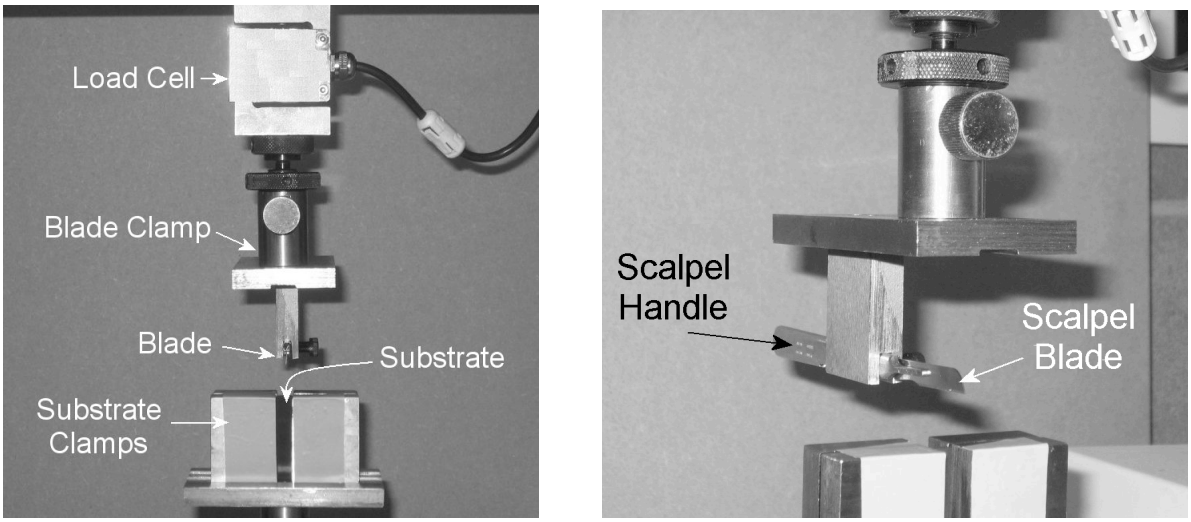

Figure 3 Experimental rig used for the cutting trials

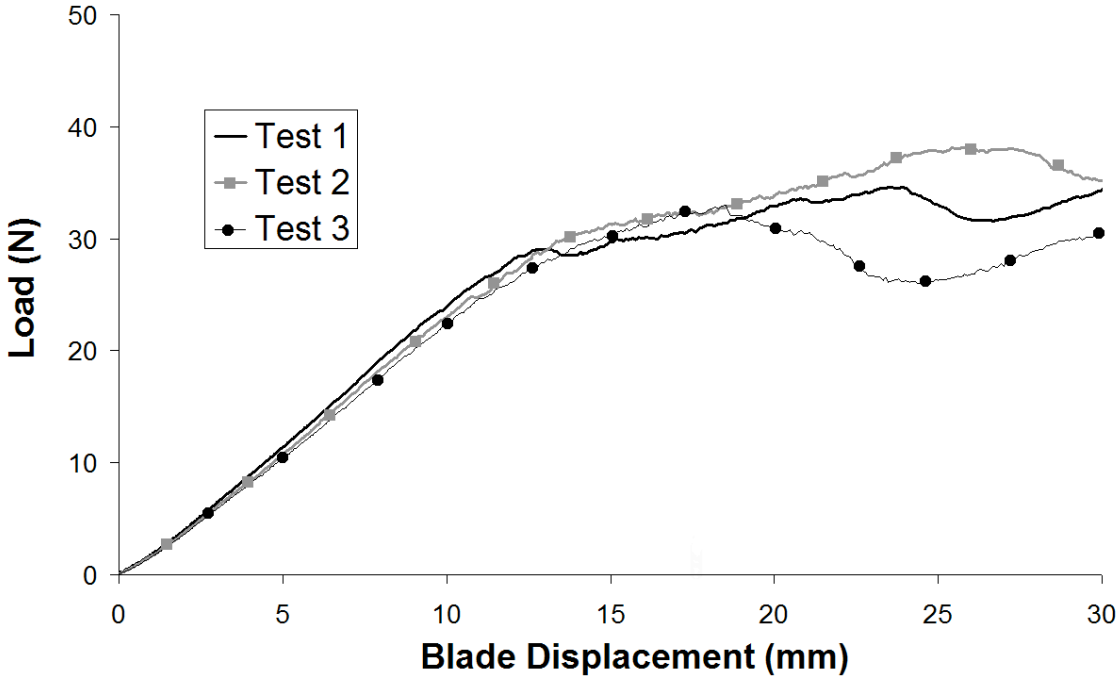

(a)

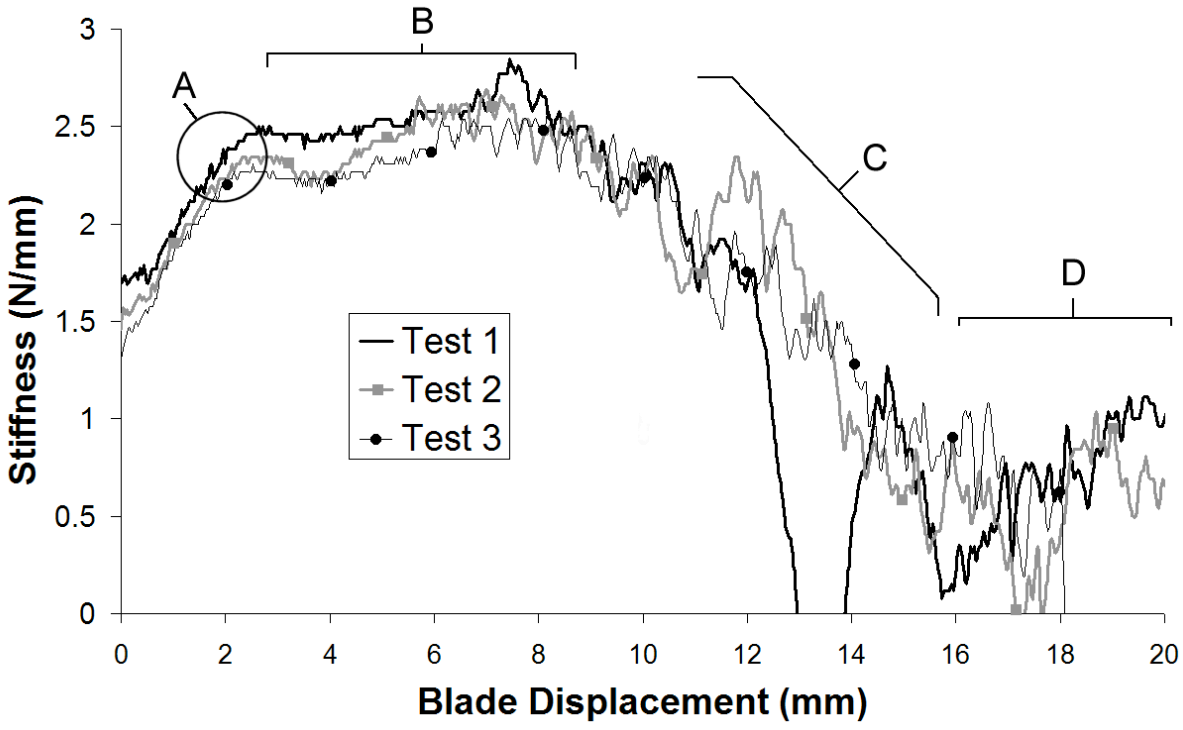

(b)

Figure 4 Indentation cutting with sharp SM blades; (a) Load-deflection curves, (b) corresponding stiffness-deflection curves

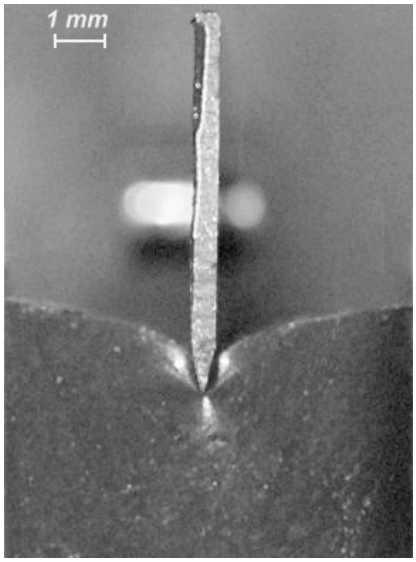

Figure 5 Photograph showing the level of blade indentation at the point of cut formation in the substrate

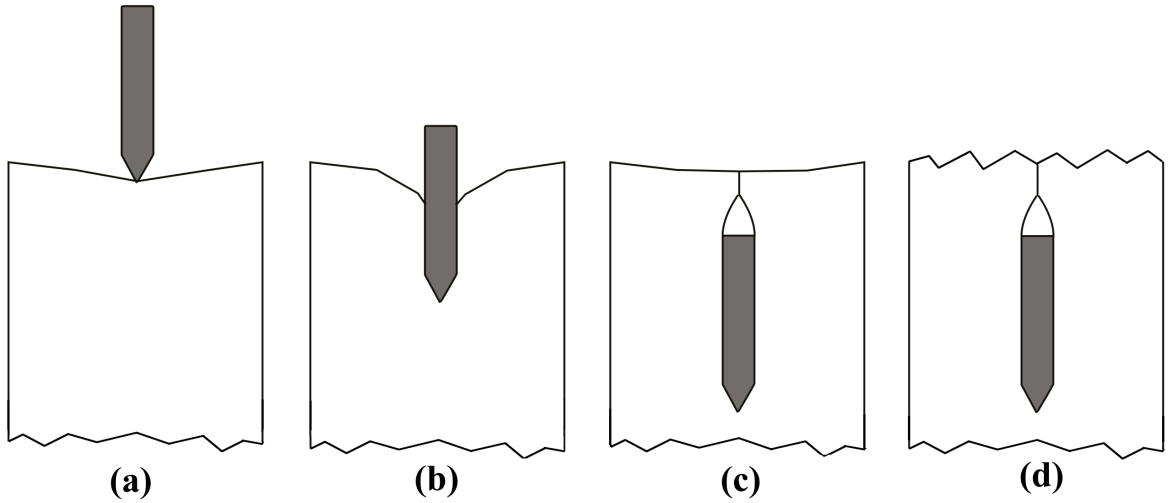

Figure 6 Different stages of the indentation cutting process; (a) Initial indentation at the point of cut formation, (b) Intermediate cutting where the cut material travels up the side of the blade, (c) onset of steady state cutting where the substrate material re-contacts above the back of the blade, (d) Steady state cutting, (a), (b), (c) and (d) correspond to locations A, B, C and D of Fig. 4(b)

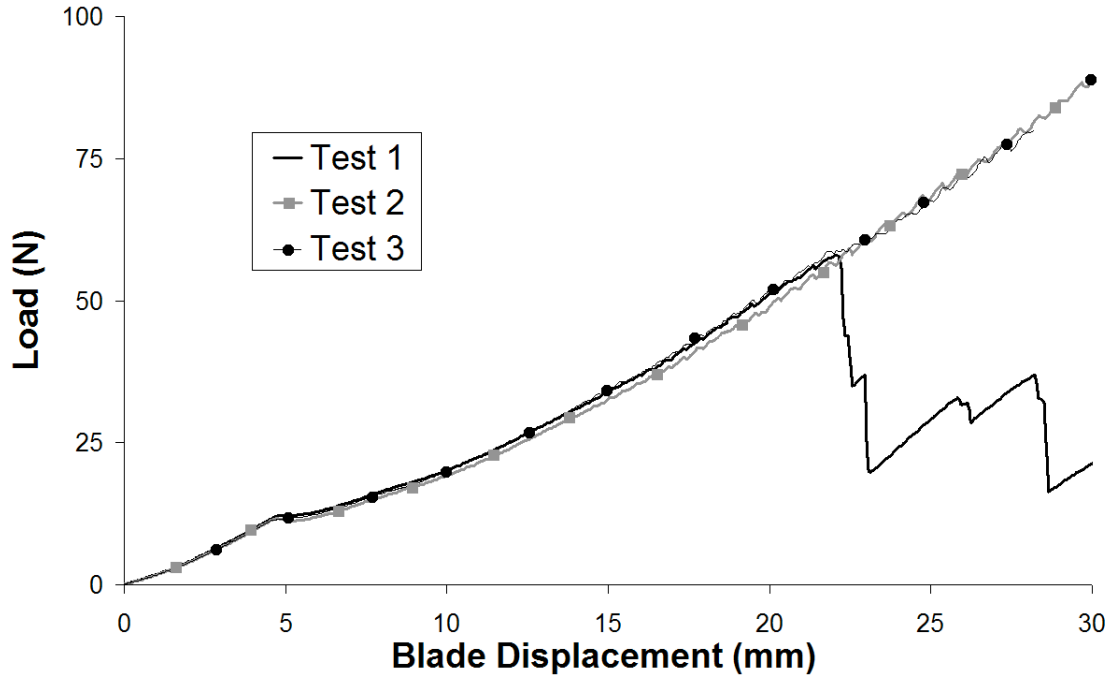

(a)

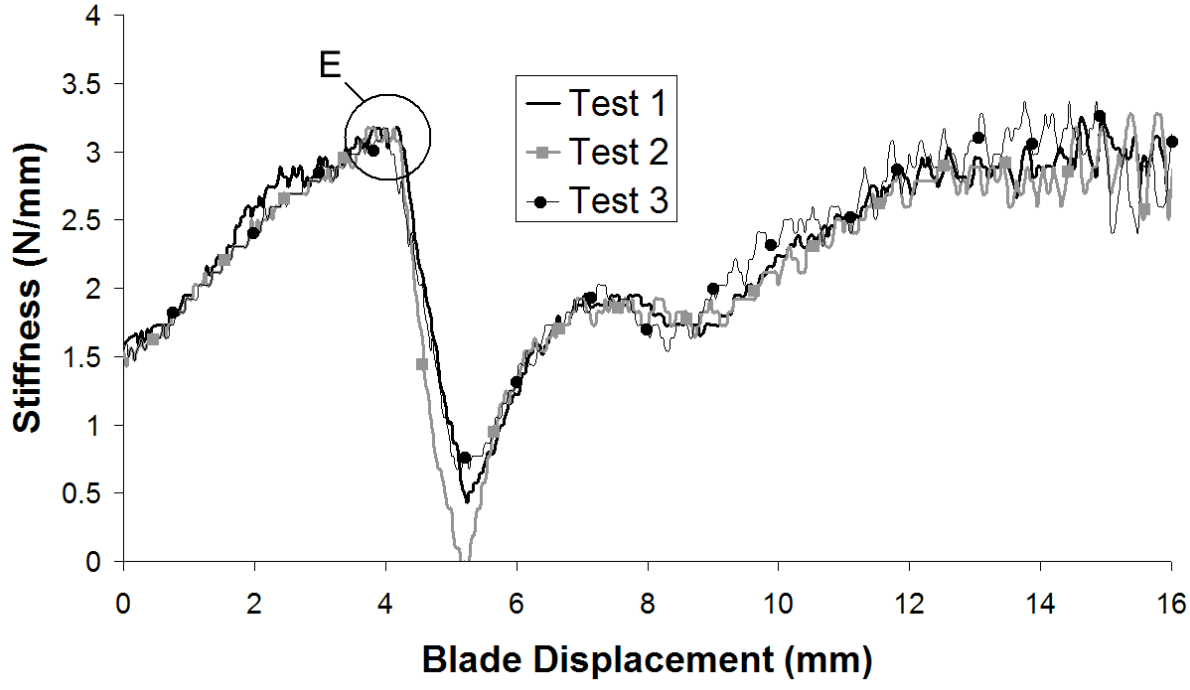

(b)

Figure 7 Indentation cutting with blunt SM blades; (a) Load-deflection curves, (b) corresponding stiffness-deflection curves

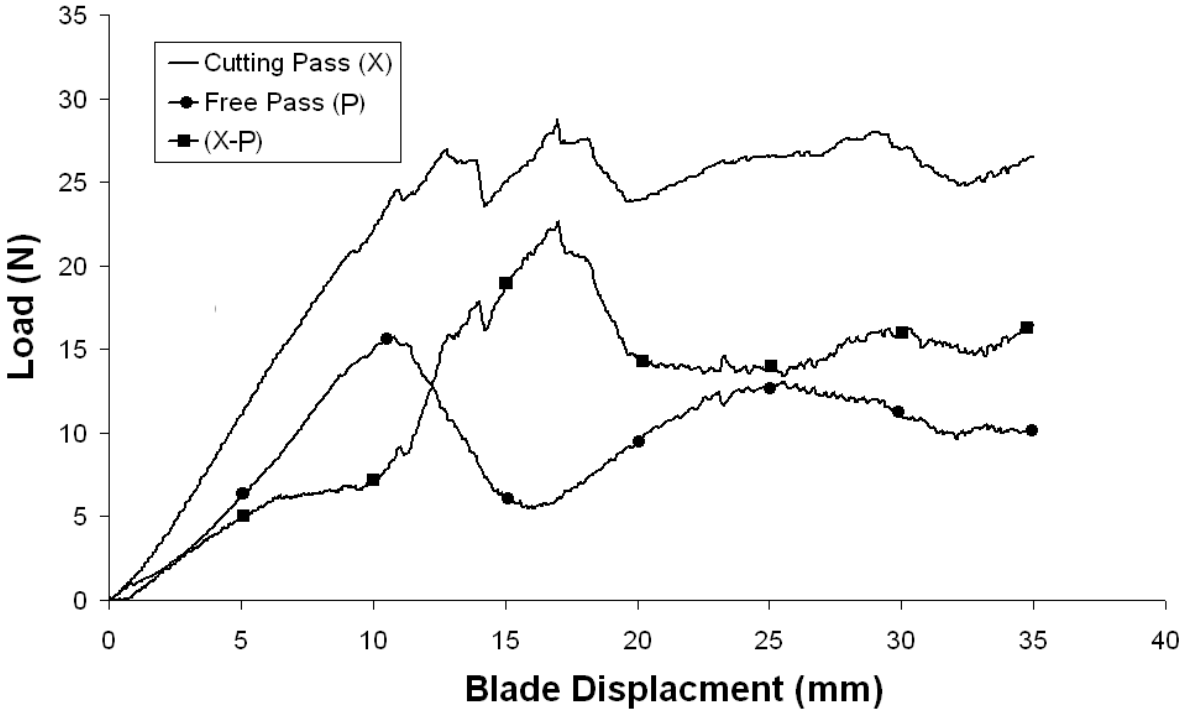

Figure 8 Load-displacement curves for a cutting pass (X), a free pass (P) and the difference (X-P)

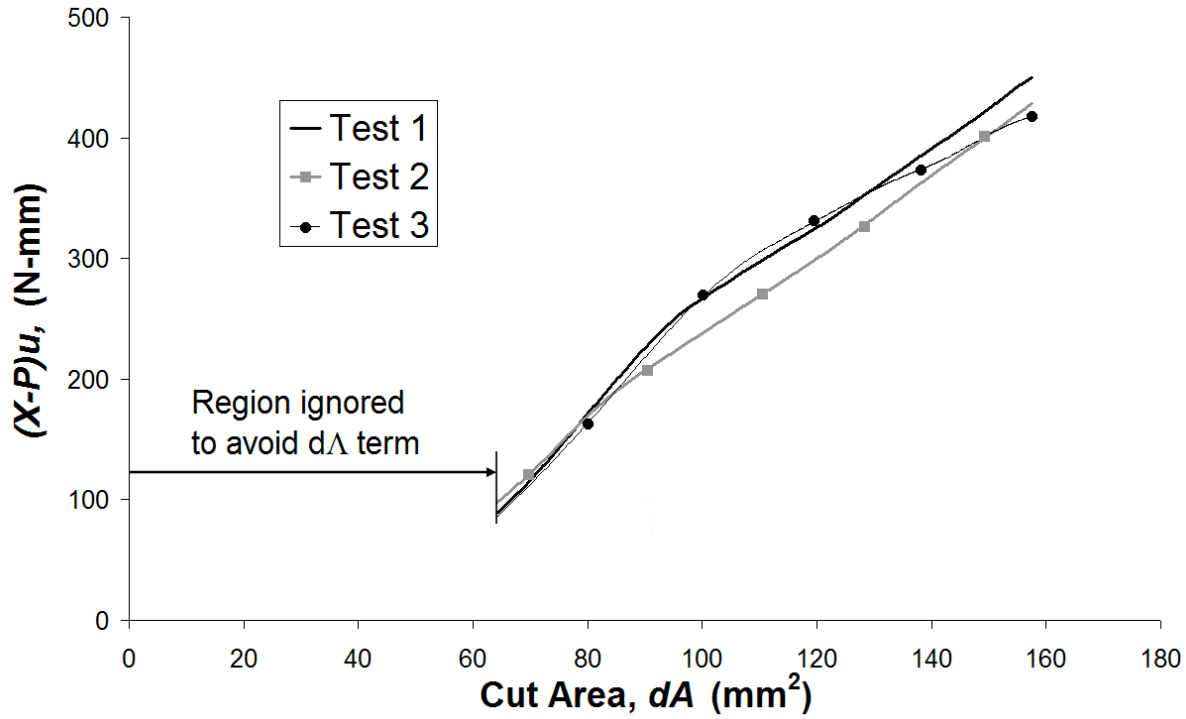

Figure 9 *(X-P)u* term as a function of cut area *dA*